Selective inactivity of pyrazinamide against tuberculosis in C3HeB/FeJ mice is best explained by neutral pH of caseum

Authors: Jean-Philippe Lanoix[1, 2], Thomas Ioerger[3], Aimee Ormond[1], Firat Kaya[4], James Sacchettini[3], Véronique Dartois[4], Eric Nuermberger[1, 5, #]

1. Center for Tuberculosis Research, Department of Medicine, Johns Hopkins University School of Medicine, Baltimore, Maryland
2. INSERM U1088, Amiens, France
3. Department of Computer Science, Texas A&M University, College Station, Texas
4. Public Health Research Institute and New Jersey Medical School, Rutgers, The State University of New Jersey, Newark, New Jersey
5. Department of International Health, Johns Hopkins Bloomberg School of Public Health, Baltimore, Maryland

Running title: Selective activity of PZA in C3HeB/FeJ mice

Corresponding author: Eric Nuermberger, MD

Mail address: Center for Tuberculosis Research, Department of Medicine, Johns Hopkins University School of Medicine, 1550 Orleans Street, Baltimore MD, 21287

e-mail: enuermb@jhmi.edu tel: +1 410 614 4225 fax: +1 410 614 8173

Word count: abstract: 170 words manuscript: 6631 words

Key words: pH; tubercles; necrotic caseum; tuberculosis; PZA; C3HeB/FeJ mice; pharmacokinetics; epithelial lining fluid;

Abstract

Pyrazinamide (PZA) is one of only two sterilizing drugs in the first-line anti-tuberculosis regimen. Its activity is strongly pH-dependent; the minimum inhibitory concentration changes by several orders of magnitude over a range of pH values that may be encountered in various in vivo compartments. We recently reported selective inactivity of PZA in a subset of C3HeB/FeJ mice with large caseous lung lesions. In the present study we evaluated whether such inactivity was explained by poor penetration of PZA into such lesions or selection of drug-resistant mutants. Despite demonstrating similar dose-proportional PZA exposures in plasma, epithelial lining fluid and lung lesions, no dose response was observed in a subset of C3HeB/FeJ mice with the highest CFU burden. Although PZA-resistant mutants eventually replaced the susceptible bacilli in BALB/c mice and in C3HeB/FeJ mice with low total CFU burdens, they never exceeded 1% of the total population in non-responding C3HeB/FeJ mice. The selective inactivity of PZA in large caseous lesions of C3HeB/FeJ mice is best explained by the neutral pH of liquefying caseum.

Introduction

Pyrazinamide (PZA) is one of only two drugs proven to be capable of shortening the duration of treatment for tuberculosis (TB) to less than 12 months (1, 2). Although it has been a part of first-line treatment regimens for 40 years, its mechanism of action remains incompletely understood (3, 4). PZA is a pro-drug that is converted to the active moiety pyrazinoic acid (POA) by a

bacterial amidase encoded by *pncA* (3). The MIC of both PZA and POA against *M. tuberculosis* is profoundly pH-dependent, changing by several orders of magnitude over the range of pH values that may be encountered *in vivo*. For example, the PZA MIC is 1000 µg/ml at a pH of 6.8, 50 µg/ml at a pH of 5.5, and theoretically as low as 5µg/ml at a pH of 4.5, which *M. tuberculosis* may encounter in the phagolysosome of activated macrophages (5-7). Thus, just as its activity *in vivo* is assumed to vary according to drug exposures at the site of infection, it also should vary significantly according to the pH at the site of infection.

The treatment-shortening, or sterilizing, effect of PZA in human TB is not readily evident in its early bactericidal activity (EBA), as measured by the average daily fall in sputum CFU count over the first 14 days of treatment. The EBA of PZA monotherapy ranges from 0.04 to 0.1 $\log_{10}$CFU/ml/day (8, 9). When administered in combination with isoniazid and rifampin, its contribution to the EBA of the regimen may be undetectable (8). Instead, the contribution of PZA is more evident during the later phase of sputum sterilization (8, 10). It is remarkable then that PZA exerts its treatment-shortening effect in the modern short-course regimen only during the first 2 months of treatment. Extending the duration of treatment has no additional benefit, in both humans and murine models (3, 11, 12).

Taken together, these characteristics suggest that PZA exerts its unique sterilizing effect against a subpopulation of tubercle bacilli residing in one or more specific compartments where the pH is sufficiently low to make the bacilli more susceptible to PZA than to other drugs. Where such subpopulations reside remains incompletely understood. It has been proposed that PZA acts against bacilli in inflammatory lung lesions where the pH is presumed to be acidic (e.g., 5.5-6.0) initially and then to increase as the lesions resolve with effective treatment (13). Alternatively,

68 the acidic milieu may persist but the bacillary sub-population that resides in that milieu making
69 it more susceptible to PZA than to another first-line drug (e.g., rifampin), may simply be
70 eradicated after 2 months of first-line therapy.

71 Active TB in humans is characterized by a variety of lesion types in which *M. tuberculosis*
72 encounters different microenvironments. Although no single non-clinical model of TB
73 recapitulates all aspects of human TB, existing models may be used in a complementary fashion
74 to better understand the impact of lesion type and resultant microenvironmental conditions on
75 the action of PZA in human disease (14, 15). Based on pharmacodynamics studies in an *in vitro*
76 hollow fiber model of TB, Gumbo et al proposed that PZA exerts its sterilizing effect against
77 extracellular bacilli because PZA accumulates to concentrations high enough to produce its
78 observed EBA at pH of 5.8 only in alveolar epithelial lining fluid (ELF) (16), and not inside
79 alveolar macrophages (17). However, there is no direct evidence that the ELF or the caseous
80 material inhabited by extracellular *M. tuberculosis in vivo* is indeed this acidic. Moreover, PZA
81 clearly exerts substantial bactericidal and sterilizing activity against established *M. tuberculosis*
82 infection in BALB/c mice, where the infecting bacilli are virtually all intracellular. In fact,
83 bactericidal activity is evident in BALB/c mice at doses producing plasma exposures
84 approximately half those produced by standard human doses (e.g., 75 mg/kg in mice), both
85 alone and in combination with rifampin and isoniazid (18). The pronounced effect of PZA in the
86 intracellular compartment is presumably due to the more acidic milieu in the phagolysosomes
87 of activated macrophages, where the pH can be as low as 4.5 (6, 7), making PZA capable of
88 significant sterilizing effects. The key role of macrophage activation in optimizing PZA effect is

89 further supported by the poor activity of PZA in mice prior to the onset of the adaptive immune
90 response and in athymic nude mice (19, 20).

91 C3HeB/FeJ mice have recently garnered significant attention as a murine TB model because,
92 unlike BALB/c and other commonly used mouse strains, they develop caseous lung lesions in
93 response to infection with *M. tuberculosis* (21-23). As expected, bacilli in the caseous core of
94 these lesions are extracellular, while the cellular cuff of caseous granulomas and other non-
95 necrotic cellular granulomas harbor intracellular bacilli. Moreover, due to differences in the rate
96 and extent of development of caseous lesions, significant heterogeneity in the presence, size
97 and degree of liquefaction of caseous lesions is often observed between mice and between
98 lesions within the same mouse at the initiation of treatment. We recently described a surprising
99 phenomenon of dichotomous activity of PZA in C3HeB/FeJ mice (24), whereby PZA had little or
100 no detectable bactericidal activity in a subset of mice with large caseous lesions despite
101 demonstrating the expected bactericidal effect in those with less extensive disease and in a
102 parallel cohort of BALB/c mice. Based on this apparent lesion-dependent activity, we
103 hypothesized that this dichotomous effect of PZA was due to its limited activity against
104 extracellular bacilli in caseum, which comprise the majority population in C3HeB/FeJ mice with
105 large caseous lesions, but bactericidal effects on the smaller numbers of bacilli in cellular lesions
106 of BALB/c and C3HeB/FeJ mice and in the cellular cuff of necrotic granulomas of C3HeB/FeJ
107 mice. However, in C3HeB/FeJ mice with large caseous lesions, the effect against intracellular
108 bacilli is largely obscured by the limited effect on the majority bacillary population in caseum.

109 In the present study we set out to determine whether this selective inactivity of PZA in large
110 caseous lesions could be explained by reduced drug penetration, selection of PZA-resistant

mutants, or insufficiently acidic conditions for PZA activity at achievable PZA concentrations. The results indicate that the near neutral pH of liquefying caseum prevents PZA from exerting any significant bactericidal activity against the numerous extracellular bacilli in larger caseous lesions and support the concept that pronounced sterilizing effects of PZA are exerted against intracellular bacilli.

Portions of the results of this study have been presented previously at the International Workshop on the Clinical Pharmacology of Tuberculosis Drugs (Abstract No. 12, Washington, DC, September 2014), and the Interscience Conference on Antimicrobial Agents and Chemotherapy (Abstract No. A-20, Washington, DC, September 2014).

Materials and methods

Mycobacterial strains

M. tuberculosis H37Rv was used as a frozen stock prepared from a log-phase culture in Middlebrook 7H9 broth after mouse passage and was diluted in 7H9 broth supplemented with 10% OADC (Oleic acid Albumin Dextrose Catalase) before infection.

Drugs and Chemotherapy

PZA was obtained from Acros Organics (Thermo Fisher Scientific, New Jersey) and formulated for oral administration in distilled water. The daily doses were (in mg/kg) 10, 30, 100, 150, 300 and 900. The most highly concentrated dosing solutions were warmed before administration to keep PZA in solution.

131 Doses were administered once daily, 5 days/week, by oral gavage, except for the 900mg/kg
132 dose, which was administered as 450mg/kg twice daily (BID) due to solubility issues.

133 *Mouse aerosol infection*

134 All animal procedures were approved by the Animal Care and Use Committee of Johns Hopkins
135 University. Female BALB/c mice (Charles River, Wilmington, MA) and C3HeB/FeJ mice (Jackson,
136 Bar Harbor, ME) were used. Age of the mice varied between 1.5 and 10 months.

137 Mice were aerosol infected using the Inhalation Exposure System (Glas-Col, Terre Haute, IN)
138 with dilutions of a titered frozen stock of *M. tuberculosis* H37Rv to implant into the lung
139 approximately 100-250 colony-forming units (CFU) for BALB/c and 50-100 CFU for C3HeB/FeJ
140 mice. One day after infection, 4 mice from each aerosol run were humanely killed to determine
141 the number of bacteria implanted.

142 *Guinea pig aerosol infection*

143 Female Hartley guinea pigs (Charles River, Wilmington, MA) 6-7 weeks old were aerosol infected
144 with *M. tuberculosis* CDC1551 using the Madison Chamber as previously described (25).

145

146 *Pharmacokinetic studies*

147 Several pharmacokinetic (PK) studies were performed in C3HeB/FeJ mice to enable comparisons
148 with results in BALB/c mice. The single dose plasma and lung concentration-time profiles were

149 determined in both 6-7 week-old and 8-10 month-old mice. Steady state plasma and lung
150 concentration-time profiles were determined in infected 5-10 month-old mice.

151 PZA concentrations were measured in samples of plasma, epithelial lining fluid (ELF) and lung
152 lesions obtained, depending of the study, at 0.08, 0.25, 0.45, 1.5, 3, 5, 7, 12 and 17 hours after
153 PZA dosing. Three or four mice from each dose group were sampled at each time point. Plasma
154 was obtained either by tail vein bleed or by cardiac puncture performed under anesthesia by
155 isoflurane inhalation. ELF was obtained after centrifugation of bronchoalveolar lavage fluid
156 (BALF) at 400 x *g* for 5min. BALF was obtained, after anesthesia by intra peritoneal injection of
157 Ketamine (200mg/kg) + Xylazine (10mg/kg), by injection and aspiration of 300µl of phosphate
158 buffered saline (PBS) via a 20G IV catheter (ProtectIV® Plus, Smith Medical ASD, Southington,
159 CT). The procedure was performed under visual control using an optic fiber (UV/VIS Fiber
160 0.22NA, 400µm; Edmund Optics, Barrington, NJ) and a fiberscope light source. Lung lesions
161 were obtained by resecting single or coalescing tubercular lesions, minimizing the amount of
162 normal-appearing lung resected to obtain at least 20mg of tissue. Lungs were rinsed in cold PBS
163 and lesions were resected on dry ice to prevent PZA diffusion or degradation.

164 Samples were frozen at -80°C before being shipped to the Dartois laboratory, Rutgers New
165 Jersey Medical School, for quantification.

166 *Quantification of PZA in samples*

167 PZA standards were obtained from Acros Organics (Thermo Fisher Scientific, New Jersey).
168 Analytes of interest were extracted by diluting 50µL of mouse serum with 50µL of
169 acetonitrole:water (1:1), and 450µL of methanol:acetonitrile (1:1) containing 0.5µg/ml of

pyrazinamide-^{15}N,d3 or pyrazinecarboxylic acid-d3 (Toronto Research Chemicals, Inc) as internal standards. The mixture was vortexed and centrifuged, and 200µL of the supernatant was recovered for analysis. LC/MS-MS analysis was performed with an Agilent 1260 system coupled to an AB Sciex 4000 Q-trap Mass Spectrometer (positive mode electrospray ionization), and an Agilent column SB-C8, 4.6 x 75mm, 3.5µm, with the column temperature fixed at 24 °C. Mobile phase A was 0.1% formic acid in 100% H_2O and mobile phase B was 0.1% formic acid in 100% acetonitrile. Injection volumes were routinely 2µL. The Mass Selective Detector was set to MRM (multiple reaction monitoring) mode using positive polarity ionization, monitoring for the ions of interest (m/z 124.0/81.1 for PZA) and the internal standard (m/z 296/215). The lower limit of quantification was 0.2µg /ml.

The urea method was used to correct for dilution of ELF by PBS in BALF samples, as previously described (16). Thus the concentration of PZA in ELF (Z_{ELF}) was derived from the following relationship: $Z_{ELF} = Z_{BAL} \times (V_{BAL}/(V_{BAL} \times (U_{BAL}/U_{PLA})))$ where Z_{BAL} is the concentration of PZA measured in BALF, V_{BAL} is the volume of BALF, U_{BAL} is the concentration of urea in BALF, and U_{PLA} is the concentration of urea in plasma. Five µl of plasma and 20µl of ELF were used with the QuantiChrom® urea assay kit (Gentaur, San Jose, CA), following manufacturer's instructions.

PK parameters (area under the concentration-time curve (AUC_{0-t}, $AUC_{0-\infty}$), Cmax, half-life) were calculated from mean concentration data using Microsoft Excel (Office 2010, Microsoft Corp, Redmond, WA). AUC was calculated using the linear trapezoidal rule. Half-life and elimination rate constant were calculated by linear regression using semi-logarithmic concentration versus

time data. Concentration values below the lower limit of quantification were excluded from the pharmacokinetic evaluation.

Pharmacodynamics study

To determine dose-ranging efficacy of PZA, 60 BALB/c and 60 C3HeB/FeJ 6-week-old mice received 10, 30, 100, 300 and 450BID mg/kg of PZA for up to 8 weeks, beginning 6 weeks after infection. Treatment efficacy was assessed on the basis of lung CFU counts determined after 3 and 8 weeks of treatment. Serial dilutions of whole lung homogenates were plated on selective Middlebrook 7H11 agar (Becton Dickinson, Franklin Lake, NJ). Plates were incubated for 6 to 8 weeks at 37°C before determining final CFU counts. At the 8 week time point, quantitative cultures were performed with 0.5ml of lung homogenates on the same 7H11 agar supplemented with 900 mg/L of PZA (which is 3-6 times the MIC against the parent H37Rv strain on this media).

Whole genome sequencing of PZA-resistant mutants

Genomic DNA extraction procedures were adapted from a previously described cetyltrimethyl ammonium bromide (CTAB)-lysozyme method (26). From 1 to 5 colonies per mouse were picked from PZA-containing plates and streaked on 7H11 agar to amplify the clone. Colonies were scraped and suspended by bead-beating (2mm sterile beads) in 5ml of PBS. Three ml of supernatant was centrifuged for 2 min (3340 x *g*) before the pellet was heat killed (30min at 80°C) in 200µL of Tris-EDTA buffer (TE buffer, Gaithersburg, MD). After 5 min of centrifugation (3340 x *g*), the pellet was incubated at 37°C overnight in 100µL of lysozyme. The extract was incubated at 65°C twice for 10 min, once after addition of 20 µl of 5% sodium dodecylsulfate

(Bio-Rad, Hercules, CA) and 20 µl of 1mg/ml Proteinase K (Thermo Scientific, Waltham, MA), and once after addition of 20 µl of 3M NaCl and 10 µl CTAB/NaCl solution. After adding chloroform:isoamylalcohol (24:1, v:v) the solution was centrifuged for 8 min at 15680 x *g*. The top layer was transferred in another tube containing 340µl of ice cold isopropanol before precipitating nucleic acids at -20°C for 30 minutes. After another centrifugation at 15680 x *g* for 15min, the pellet was washed with ice cold 70% ethanol and then dissolved in 20µl of pure water after a second centrifugation.

Samples were sequenced on an Illumina GAIIx next-generation sequencer. DNA samples were prepared for sequencing using the standard genomic DNA sample preparation protocol (Illumina Inc., San Diego, CA). Paired-end data was collected with a read length of 54+54 bp. Base-calling was performed using RTA 1.9.35, and genome assembly was carried out using a comparative assembly technique as described in (27), using the genome of H37Rv as a reference sequence. The mean depth of coverage over all samples was 29.5x.

Assessment of pH of the lesions

The pH of liquefied caseum from selected lesions of more than 3mm diameter was measured with a 16G needle tip micro-pH comb electrode (Thermo Scientific Orion, Chelmsford, MA) and a benchtop pH meter Mettler Toledo FE20 (Business Unit Analytical, Schwerzenbach, Switzerland). The probe was inserted directly into the tubercle to measure the pH of the liquefied material.

Data Analysis

Lung CFU counts (x) were log-transformed as $\log_{10}(x + 1)$ before analysis. Group mean CFU counts after 2 months of treatment were compared using one-way analysis of variance with GraphPad Prism v.5 (GraphPad Software, San Diego, CA) and Bonferroni's posttest to adjust for multiple comparisons, as appropriate. A non-linear dose-response regression was used to calculate PZA dose-response using the same software.

Results

Pharmacokinetics of PZA

Uninfected mice

Total daily doses from 10 to 900mg/kg of PZA were administered. As stated in the methods section, PZA was administered orally once a day, except for 900 mg/kg which was administered as two 450mg/kg doses given 12 hours apart (BID). PZA concentrations were measured in plasma and ELF.

As shown in Figure 1 uninfected C3HeB/FeJ mice had at least dose proportional (possibly supra-proportional) exposures in plasma and also in ELF (data not shown). The PK parameter values for plasma are presented in Table 1 and were comparable to previous published results (28). The concentrations produced by the lowest doses of PZA were not quantifiable in ELF because of the high dilution factor. The median ratio of ELF/plasma concentrations ranged between 0.9-3 at 3h and tended to increase slightly over time to 1.2-3.7 independently of dose (except for 300mg/kg, where the ratio decreased) (Table 2).

Infected mice

Infected C3HeB/FeJ mice received 150mg/kg once daily or 450mg/kg BID doses of PZA for 3 days or 4 weeks before PZA concentrations were measured in plasma, ELF and tubercular lesions. No major difference was observed in plasma PZA concentrations between infected and uninfected mice, although AUC and C_{max} were numerically lower in infected mice receiving 450mg/kg BID compared to uninfected mice (Table 1). Plasma PK parameters in infected

C3HeB/FeJ mice were comparable to past results in infected BALB/c mice (28) (Table 1). The dose proportionality was conserved both in plasma (Figure 2) and in ELF. In ELF, PZA concentrations seemed to be more variable between mice and between experiments than what was observed in plasma (data not shown). The ratio of PZA concentrations in ELF/plasma in infected mice was similar to that observed in uninfected mice (Table 2).

The concentrations of PZA in lesions largely mirrored concentrations in plasma (Figure 2). The measurements from a representative large necrotic granuloma sampled 7h after a dose of 150mg/kg were similar for the capsule and the liquefied caseum (2.68 and 1.76µg/ml respectively). When comparing PZA concentrations in lesions of mice with large necrotic granulomas (>3mm) and mice without such lesions, at the same time points, means tended to be higher in larger lesions than in smaller lesions. For example, in samples obtained 90min after a 150mg/kg dose, 3 large lesions had a mean PZA concentration of 105.1µg/ml whereas 3 smaller lesions averaged 80.1µg/ml, but the difference was not statistically significant (p=0.07). In samples obtained 7h after the same dose, 3 large lesions had a mean PZA concentration of 3.5µg/ml whereas 2 smaller lesions averaged 2µg/ml (p=0.055). The median ratios of lesion/plasma concentration were 0.8 and 0.7 at 1.5h for 150mg/kg and 450mg/kg BID respectively, and remained stable between 0.8-1.2 over time.

Pharmacodynamics of PZA

In the dose-ranging efficacy study, BALB/c and C3HeB/FeJ mice received daily doses ranging from 10 to 450 BID mg/kg of PZA for 3 to 8 weeks. Mean (SD) CFU counts at the start of treatment (D0) were 6.86 (0.17) for BALB/c mice and 7.09 (0.12) for C3HeB/FeJ mice. As

278 previously described (24), PZA was associated with a dichotomous dose-response relationship in
279 C3HeB/FeJ mice but not in BALB/c mice. Dose-proportional bactericidal activity was observed in
280 BALB/c mice and in most C3HeB/FeJ mice at each time point. At doses of 100 mg/kg and above,
281 the bactericidal effect size increased between 3 and 8 weeks of treatment. After 8 weeks,
282 increasing the dose from 30 to 300mg/kg increased the log-kill by 2 $\log_{10}$, and increasing the
283 dose from 300 mg/kg to 450 mg/kg BID increased the log-kill by another 2 $\log_{10}$ in both mouse
284 strains (Figure 3). However, no dose response effect was observed in a subset of C3HeB/FeJ
285 mice, even after 8 weeks of treatment (Figure 3). CFU counts after 8 weeks in these poor
286 responders were one-half to one log lower compared to week 3, so some modest activity could
287 not be excluded. Excluding these outliers, the goodness of fit of the logarithmic dose-response
288 curve was r^2=0.92 at week 3 and 0.87 at week 8; the maximum effect (E_{max}) at week 3 was
289 3.27$\log_{10}$ and the dose producing 50% of the E_{max} (EC_{50}) was 128.4mg/kg (95% confidence
290 interval [CI] = 58.32-281.2). Similar curve fits and parameters were observed in BALB/c mice,
291 e.g., the goodness of fit was r^2=0.87 and 0.98 at weeks 3 and 8 respectively; E_{max} was 3.06$\log_{10}$
292 and EC_{50} was 139.6mg/kg (95%CI = 61.26-318.1) at week 3.

293 *Selection and characterization of PZA-resistant mutants*

294 After 8 weeks of treatment, 11 (37%) of 30 BALB/c mice had colonies on PZA-containing plates,
295 compared to 18 (75%) of 24 C3HeB/FeJ mice ($p < 0.01$). Resistance among BALB/c mice was only
296 observed at PZA doses ≥100mg/kg, whereas resistance among C3HeB/FeJ mice was observed at
297 all dose levels. Despite the proclivity towards selection of resistant mutants in C3HeB/FeJ mice,
298 replacement of the PZA-susceptible bacillary population with PZA-resistant mutants did not
299 explain the poor activity of PZA in those with the highest CFU counts at the end of treatment.

300 Indeed, the greatest proportion of PZA-resistant CFU compared to total CFU was among those
301 C3HeB/FeJ mice receiving the highest PZA doses in which the greatest bactericidal activity was
302 observed (where up to 100% of the total population was resistant to PZA). On the contrary,
303 among mice in which PZA did not exhibit bactericidal activity, PZA-resistant mutants remained ≤
304 1% of the total CFU (Figure 4). Nevertheless, both the absolute number and the proportion of
305 bacteria resistant to PZA tended to increase with dose among the poorly responding C3HeB/FeJ
306 mice, indicating that PZA was likely exerting a bactericidal effect against drug-susceptible bacilli
307 and promoting selective amplification of resistant mutants within a minority sub-population
308 within these mice, likely in the intracellular compartment. The mean CFU counts of PZA-
309 resistant mutants were not statistically different between the 2 mouse strains (p=0.89, 0.11,
310 0.17 for 100, 300 mg/kg and 450 mg/kg BID doses respectively).

311 Although colonies from each mouse harboring resistant mutants were processed for whole
312 genome sequencing, only 79% of colonies selected (20/27 for BALB/c and 53/65 for C3HeB/FeJ)
313 were actually sequenced due to a variety of technical difficulties.

314 With one exception, all sequenced colonies isolated on PZA-containing media had mutations in
315 *pncA*, confirming the utility of employing3-6xMIC PZA concentrations in standard 7H11 agar (pH
316 6.8) for isolating resistant mutants. In most cases, different colonies from the same mouse
317 harbored the same *pncA* mutation. Out of 13 C3HeB/FeJ mice with several colonies sequenced,
318 2 mice had 3 or more colonies with differing mutations in *pncA*, whereas 7 mice had 2 colonies
319 with either of 2 different mutations, and 4 mice had colonies sharing only one mutation. Among
320 5 BALB/c mice with several colonies sequenced, 2 mice had colonies with either of 2 different
321 *pncA* mutations and 3 mice had colonies sharing only one mutation. Table 3 catalogs the

mutations identified, most of which have previously been reported as clinically relevant mutations likely to confer PZA resistance (29, 30). Notably, deletions spanning multiple open reading frames were quite frequent (8/29 for C3HeB/FeJ vs. 2/10 for BALB/c). Apart from deletions, seven different mutations in *pncA* were identified in BALB/c mice and 20 in C3HeB/FeJ mice. Each *pncA* mutation was observed in only one mouse. The only colony without a *pncA* mutation was selected in a C3HeB/FeJ mouse treated with 300mg/kg and harbored only an A3311T mutation in Rv3350c (PPE56). Three other colonies isolated from the same mouse had this mutation as well as identical 2 bp deletions in *pncA*. The fifth colony had no mutation in Rv3350c, only a different (G108R) mutation in *pncA*.

pH assessment

We recently reported that the pH of liquefied caseous material from lesions in C3HeB/FeJ mice was 7.39 ± 0.096 (range 7.19 - 7.54) (24). To extend our evaluation to another non-clinical species, we measured pH in 12 different lesions in 4 untreated guinea pigs infected for 13 weeks. An average pH of 7.23 ± 0.17 (range 6.99 – 7.52) was found, only slightly lower than that of the adjacent normal-appearing lung (7.35 ± 0.22).

Antimicrobial Agents and Chemotherapy

338 **Discussion**

339 In a previous study we observed that PZA had limited activity in a subset of C3HeB/FeJ mice
340 with large caseous lesions and hypothesized that this was due to the neutral pH of the liquefied
341 caseum in such lesions (24). In this study we bring additional evidence in support of this
342 hypothesis by demonstrating that neither poor distribution of PZA into caseous lesions nor
343 selection of PZA-resistant mutants explains the limited PZA activity and the observed lack of
344 dose-response effect.

345 Indeed PZA exposures increased in a dose proportional fashion in plasma and ELF in both
346 uninfected and infected mice and, at doses of 100 mg/kg or higher, met or exceeded plasma
347 exposures observed in humans receiving PZA at doses recommended for TB treatment (16, 31).
348 Moreover, PZA concentrations in the caseous lesions of infected C3HeB/FeJ mice also increased
349 dose-proportionally and were, on average, 67% of the concurrent plasma concentration, a ratio
350 similar to that recently observed in a rabbit TB model and consistent with evidence that PZA
351 diffuses readily through caseum (32-34). To our knowledge, this is the first report of PZA
352 concentrations in ELF in mice. Conte et al (16) described higher concentrations of PZA in ELF
353 relative to plasma in uninfected human subjects (ratio ELF/plasma concentration of 13-24) than
354 we observed in infected mice, except for the median ratio of 22.8 we observed in mice sampled
355 12 hours after a 150mg/kg dose. This discrepancy may be due in part to the higher systemic
356 clearance of PZA in mice allowing less accumulation in ELF compared to humans. However,
357 determination of ELF concentrations of rapidly diffusing small molecules like PZA is also
358 technically challenging because small differences in dwell time during bronchoalveolar lavage
359 can introduce large differences in concentration due to rapid drug redistribution from tissue

into lavage fluid (35). If the drug in question distributes faster than urea, its ELF concentration could be over-estimated as the dwell time of the lavage fluid increases. Importantly, infection did not appear to increase the distribution of PZA into the ELF.

As indicated by the lack of a dose-response effect in C3HeB/FeJ mice with large caseous lesions, achieving higher PZA concentrations are useful only if the pH of the actual lung compartment inhabited by *M. tuberculosis* is sufficiently acidic for PZA to exert its effect. According to Zhang's model, intrabacillary accumulation of the active POA moiety increases inversely with the pH of the milieu (3). At neutral pH, the PZA MIC against *M. tuberculosis* H37Rv may exceed 1600 µg/ml (5), which is 3-4 times higher than the highest average steady state ELF concentrations observed in uninfected mice in this study or at 4 hours post-dose in uninfected human subjects administered 1 g daily for 5 days (16), as well as in infected mice receiving a PZA dose (150 mg/kg) that most closely approximates plasma AUCs observed in patients receiving recommended PZA doses. Only the C_{max} in the ELF of infected mice receiving 450 mg/kg BID approached the MIC at neutral pH.

Against cultures of *M. tuberculosis* H37Rv adjusted to a pH of 5.8 in an *in vitro* hollow fiber model of TB, Gumbo et al established that human-like exposures producing a PZA AUC of approximately 1500 µg.h/ml (i.e., AUC/MIC of 120 x MIC of 12.5) produces the same 0.11 log_{10}CFU/ml/day fall in CFU counts that was observed in 14-day clinical EBA trials (8, 17). Although the typical plasma AUC produced by standard PZA doses is only 300-500 µg.h/ml, the degree to which PZA was shown to accumulate in ELF provided a parsimonious explanation for sufficient target attainment in lung cavities, leading the authors to conclude that, because PZA does not accumulate above plasma concentrations inside cells, PZA most likely exerts its

sterilizing activity against extracellular bacilli. However, the bactericidal and sterilizing activity of doses producing clinically relevant plasma PZA AUC values in commonly used mouse strains, in which virtually all bacilli are found intracellularly, is well demonstrated (11, 18, 36). In the present study, we found that after 15 doses of PZA administered to BALB/c mice, the EC_{50} of approximately 150 mg/kg produced a 0.102 $\log_{10}$CFU/dose reduction. The mean plasma AUC produced by this dose is 388 µg.hr/ml. Thus, a dose producing similar plasma AUC in BALB/c mice and humans produces similar EBA at exposures that are approximately one-quarter of the exposure required for the same effect in the hollow fiber system at pH of 5.8. The lower exposures needed to observe the same kill in mice compared to the hollow fiber would be explained if the pH in infected murine macrophages is closer to 5.0, a level that is attained by activated macrophages (7, 37).

If extracellular bacilli are a target of PZA's sterilizing activity, then the pH of the ELF or caseum in which they are found should be sufficiently low for the expected PZA concentrations to be active. For example, a pH of 5.8 was studied in the hollow fiber model (17). The technique of sampling ELF via BAL makes it difficult to measure ELF pH. However, it is possible to measure the pH of airway lining fluid *in vivo*. The pH of the tracheal lining fluid of anesthetized mice was reported to be 7.1 (38). Similarly, a study using a bronchoscopically directed pH electrode reported the pH of subsegmental bronchi to be 6.6 in humans (6.48 in patients presenting with bacterial pneumonia) (39). Our finding of a more neutral pH in caseum from C3HeB/FeJ mouse and guinea pig tubercles extends previous work in rabbits showing an increase in pH of caseum (from 6.4 to 7.4) as lesions mature, caseate and liquefy (40). We are aware of only one report of the pH of caseum from human cavities which described the pH of resected cavity tissue

404 homogenates as ranging between 6.1 and 7.4, but noted that the pH was 6.8 or above in 15 out
405 of 17 lesions (41). This report is well in line with the aforementioned results from animal
406 models. Taken together, these data run counter to the prevailing notion that caseum is acidic
407 and make the assumption that extracellular bacilli routinely encounter conditions of pH ≤ 6.5
408 rather tenuous (17).

409 The remarkable dichotomous activity of PZA in C3HeB/FeJ mice in the present study confirms
410 and extends our prior results (24). It also is consistent with the important role of pH in the
411 action of PZA. Among those mice with less severe disease, the pharmacodynamics of PZA were
412 similar to that observed in BALB/c mice, suggesting similar conditions wherever bacilli are found
413 intracellularly in C3HeB/FeJ mice, such as in small cellular granulomas or in the cellular cuff of
414 caseous granulomas. Based on the exposure-response relationship defined in the hollow fiber
415 model (17), the PZA exposures attained inside mouse macrophages would not be expected to
416 exert a bactericidal effect comparable to the EBA in humans unless the pH in the macrophage
417 compartment was below 5.8 and closer to 5.0, a value attainable in activated macrophages (7).
418 On the other hand, in those C3HeB/FeJ mice with large caseous lesions where the pH
419 approaches 7.4 (24), little or no bactericidal activity of PZA was observed despite attaining
420 plasma AUCs that are 3-5 times those produced in plasma at typical human doses but similar to
421 the AUC associated with a 0.11 $\log_{10}$ CFU reduction per day at pH of 5.8 in the hollow fiber
422 experiments (17). Moreover, the estimated PZA AUC in these lesions of approximately 850
423 µg.h/ml is the same as that associated with a 2 log kill over 28 days in the hollow fiber
424 experiments. Taken together, these results are consistent with the idea that local pH has a
425 profound effect on PZA activity.

426 The facts that PZA exerts its sterilizing contribution during the first 2 months of treatment in the
427 current first-line regimen and that patients unable to take PZA can still be cured when rifampin-
428 containing regimens are given for 9 months rather than the usual 6 months with PZA (42),
429 suggests that the bacillary population eradicated by PZA is not susceptible only to PZA, just
430 more susceptible to PZA than to rifampin, and that this population is of a limited size. When the
431 pH is 6.5 and above, it is unlikely that PZA exposures routinely achieved in TB patients will
432 produce the kind of bactericidal effect that will lend significant additive sterilizing activity to the
433 first-line regimen. The high pH of the caseum lining the cavity wall likely explains the limited
434 contribution of PZA to the activity of the first-line regimen over the first 14 days of treatment.
435 There is ample evidence however, that PZA contributes to the sterilization of sputum cultures
436 later in the initial phase in patients receiving the first-line regimen, including recent evidence
437 that this contribution is exposure-dependent (10). While the poor results in mice with large
438 caseous lesions seems inconsistent with the well-known treatment shortening potential of PZA
439 in humans, the results may be quite consistent if one considers its sterilizing activity is only
440 evident in the context of combination therapy. Our results suggest that while other drugs like
441 rifampin and isoniazid eradicate the bacilli in caseous material, PZA eliminates a subpopulation
442 that is likely residing inside macrophages, in phagolysosomes at low pH, where achievable PZA
443 concentrations exceed the local MIC. The pH dependence of PZA activity, the near neutral pH of
444 caseum across species, and the dramatic lesion-dependence of PZA activity in C3HeB/FeJ mice is
445 compelling evidence that PZA exerts its most prominent sterilizing effects against intracellular
446 bacilli. This model is not mutually exclusive with the model proposed by Gumbo et al in which
447 PZA exerts activity against extracellular bacilli in sufficiently acidic environments. Rather, given

448 the remarkable heterogeneity observed in human TB, these models might be considered
449 complementary. Further studies to evaluate the sterilizing activity of PZA in combination
450 therapy and to isolate the lesions in C3HeB/FeJ mice in which PZA exerts a sterilizing effect are
451 warranted.

452 We found that, like C3HeB/FeJ mice and rabbits, guinea pigs develop necrotic lesions with
453 neutral caseum by 13 weeks post-infection. Despite this, PZA has been reported to have
454 bactericidal activity in guinea pigs (36). This apparent discrepancy may be explained by the fact
455 that examinations of lung histopathology revealed only poorly formed granulomas and limited
456 necrosis at the time of treatment initiation (4 weeks post-infection) and active doses of PZA
457 were associated with reduced numbers and size of granulomas (at 8 weeks post-infection) (36).
458 Thus, it is likely that PZA exerted its bactericidal effect against bacilli under low pH conditions
459 inside activated macrophages rather than inside caseous regions. Further studies of PZA activity
460 against more established disease in guinea pigs are warranted to test this hypothesis.

461 PZA resistance was not the explanation for the dichotomous activity of PZA in C3HeB/FeJ mice,
462 since resistant mutants never replaced the sensitive population in the mice with worst response
463 to PZA. However, it is interesting to see that selective amplification of PZA-resistant mutants
464 occurs more readily, including at lower doses, in C3HeB/FeJ mice compared to BALB/c mice
465 (18/24 vs 11/30 respectively). Many C3HeB/FeJ mice receiving doses ≥ 100 mg/kg for 8 weeks
466 harbored more than 0.1% PZA-resistant CFU, including mice in which the week 8 CFU count was
467 likely not significantly lower than the D0 CFU count. This is evidence that, even when PZA was
468 not exerting bactericidal effects on the largest population of bacilli in the large caseous lesions,
469 it was exerting significant bactericidal activity against PZA-susceptible bacilli and selectively

amplifying PZA-resistant mutants in smaller granulomas and cellular lesions similar to those in BALB/c mice. The limited effect of PZA in liquefied caseum, where the highest bacterial counts are observed, may help to explain why PZA resistance typically emerges only after resistance to rifampin and isoniazid, and why PZA is not very effective at preventing the emergence of resistance to these and other companion agents that are bactericidal in that compartment (43). However, additional experiments comparing the selection of mutants resistant to PZA and to companion agents in large caseous lesions versus the rest of the lung are needed to confirm these results.

PZA resistance was explained by *pncA* mutations in all mice. Virtually all of these mutations have been described in PZA-resistant clinical isolates and most of them were found only in PZA-resistant isolates, adding to the evidence presented here that these mutations confer PZA resistance (30). Therefore, C3HeB/FeJ mice may be an excellent model to study factors associated with the selection of PZA-resistant mutants and the clinical significance of specific mutations. It is noteworthy that large multigenic deletions including *pncA* were observed in some PZA-resistant isolates from mice. Multigenic deletions are rare among reported clinical isolates (44, 45). However, they may be more difficult to detect by selective sequencing approaches commonly used with clinical isolates.

Our study has important limitations. Firstly, we did not plate large caseous lesions in C3HeB/FeJ mice separately from the rest of the lung, which prevented specific confirmation of where the selective killing of PZA-susceptible bacteria and amplification of PZA-resistant mutants was

491 occurring. Secondly, in extrapolating the pH of TB lesion compartments from mice and other
492 animal models to humans, we are limited by the scant data available on the pH of human
493 caseum and the intracellular compartments inhabited by phagocytosed bacteria *in vivo*.
494 Although further confirmation of the pH of human caseum is needed, the available data
495 presented above suggest a similar pH across species. Although there is evidence that
496 macrophages activated with interferon-gamma *in vitro* deliver *M. tuberculosis* to an acidic
497 compartment with a pH as low as 4.5-5.0 (7), confirmation of delivery of Mtb to acidified
498 phagosomes in a living infected host was elusive until recently (46). Still, new tools are needed
499 to more accurately quantify the pH of intracellular vacuoles and other lesion compartments
500 inhabited by *M. tuberculosis in vivo* in a manner that can be correlated with PZA
501 pharmacodynamics. A third limitation is that, due to the more rapid clearance of PZA in mice
502 compared to humans, the concentration-time profiles produced in our mice reproduced human
503 AUCs but did not necessarily mimic the time course of PZA concentrations in humans. As
504 mentioned above, this may be one reason for less accumulation of PZA in ELF of mice compared
505 to humans. It also may lead to discordance between the relationships of important PK/PD-based
506 exposure indices and targets to efficacy and therefore demands caution when extrapolating
507 between mice and humans or the hollow fiber model, as we have here. A final limitation of this
508 study is the high level of dilution (median=40, IQR=21-64) of ELF with PBS, which made the
509 lower limit of PZA quantification higher than that of plasma. The technical limit of quantification
510 in each sample was 0.2µg/ml, making the lower limit of quantification in ELF 4-13µg/ml.
511 Furthermore BAL was performed with 300µL of PBS rendering infeasible to duplicate samples or
512 to repeat runs when results were not within 20% of controls (1 case out of 11).

513

514 **Conclusions**

515 In this study, we confirm that PZA has variable, lesion-dependent activity in C3HeB/FeJ mice in
516 which poor PZA activity occurs in large caseous lesions due to the neutral pH of the caseum
517 therein. Such lesion-dependent activity of PZA in C3HeB/FeJ mice, like that recently
518 demonstrated for clofazimine and oxazolidinones (24, 47), promotes the C3HeB/FeJ mouse
519 model as a valuable tool for studying the influence of lesion type and microenvironment on
520 drug distribution and drug action, including the selection of drug-resistant mutants. Although
521 additional studies to evaluate the contribution of PZA to the standard first-line regimen in
522 C3HeB/FeJ mice are warranted, these results suggest that future investigations in C3HeB/FeJ
523 mice may give a more holistic and nuanced appraisal of the potential contribution of PZA to
524 novel regimens.

525

526 **Acknowledgment**

527 This work has been funded by grants from the Bill and Melinda Gates foundation (OPP1037174
528 [EN], OPP1066499 [VD]) and a supplement to the Johns Hopkins University Center for AIDS
529 Research (P30AI094189)

530 The authors thank Si-Yang Li, Jin Lee, and Fabrice Betoudji for their help during the experiments,
531 and Alvaro Ordonez and Bappaditya Dey for providing the interspecies animals. We also thank

532 Anne Lenaerts, Khisi Mdluli and Omar Vandal for valuable discussions of the results presented
533 here and the potential role of C3HeB/FeJ mice in pre-clinical drug development.

534

References

1. **British Thoracic and Tuberculosis Association.** 1976. Short-course chemotherapy in pulmonary tuberculosis. A controlled trial by the British Thoracic and Tuberculosis Association. Lancet **2:**1102-1104.
2. **British Medical Research.** 1984. A controlled trial of 6 months' chemotherapy in pulmonary tuberculosis. Final report: results during the 36 months after the end of chemotherapy and beyond. British Thoracic Society. Br J Dis Chest **78:**330-336.
3. **Zhang Y, Mitchison D.** 2003. The curious characteristics of pyrazinamide: a review. Int J Tuberc Lung Dis **7:**6-21.
4. **Shi W, Zhang X, Jiang X, Yuan H, Lee JS, Barry CE, Wang H, Zhang W, Zhang Y.** 2011. Pyrazinamide inhibits trans-translation in Mycobacterium tuberculosis. Science **333:**1630-1632.
5. **Zhang Y, Permar S, Sun Z.** 2002. Conditions that may affect the results of susceptibility testing of Mycobacterium tuberculosis to pyrazinamide. J Med Microbiol **51:**42-49.
6. **Vandal OH, Pierini LM, Schnappinger D, Nathan CF, Ehrt S.** 2008. A membrane protein preserves intrabacterial pH in intraphagosomal Mycobacterium tuberculosis. Nat Med **14:**849-854.
7. **MacMicking JD, Taylor GA, McKinney JD.** 2003. Immune control of tuberculosis by IFN-gamma-inducible LRG-47. Science **302:**654-659.
8. **Jindani A, Doré CJ, Mitchison DA.** 2003. Bactericidal and sterilizing activities of antituberculosis drugs during the first 14 days. Am J Respir Crit Care Med **167:**1348-1354.
9. **Diacon AH, Dawson R, von Groote-Bidlingmaier F, Symons G, Venter A, Donald PR, van Niekerk C, Everitt D, Hutchings J, Burger DA, Schall R, Mendel CM.** 2015. Bactericidal activity of pyrazinamide and clofazimine alone and in combinations with pretomanid and bedaquiline. Am J Respir Crit Care Med **191:**943-953.
10. **Chigutsa E, Pasipanodya JG, Visser ME, van Helden PD, Smith PJ, Sirgel FA, Gumbo T, McIlleron H.** 2015. Impact of nonlinear interactions of pharmacokinetics and MICs on sputum bacillary kill rates as a marker of sterilizing effect in tuberculosis. Antimicrob Agents Chemother **59:**38-45.
11. **Grosset J, Truffot C, Fermanian J, Lecoeur H.** 1982. [Sterilizing activity of the main drugs on the mouse experimental tuberculosis (author's transl)]. Pathol Biol (Paris) **30:**444-448.
12. **Hong Kong Chest Service/British Medical Research Council.** 1991. Controlled trial of 2, 4, and 6 months of pyrazinamide in 6-month, three-times-weekly regimens for smear-positive pulmonary tuberculosis, including an assessment of a combined preparation of isoniazid, rifampin, and

pyrazinamide. Results at 30 months. Hong Kong Chest Service/British Medical Research Council. Am Rev Respir Dis **143:**700-706.

13. **Mitchison DA, Fourie PB.** 2010. The near future: improving the activity of rifamycins and pyrazinamide. Tuberculosis (Edinb) **90:**177-181.

14. **Gumbo T, Lenaerts AJ, Hanna D, Romero K, Nuermberger E.** 2015. Nonclinical models for antituberculosis drug development: a landscape analysis. J Infect Dis **211 Suppl 3:**S83-95.

15. **Lenaerts A, Barry CE, Dartois V.** 2015. Heterogeneity in tuberculosis pathology, microenvironments and therapeutic responses. Immunol Rev **264:**288-307.

16. **Conte JE, Golden JA, Duncan S, McKenna E, Zurlinden E.** 1999. Intrapulmonary concentrations of pyrazinamide. Antimicrob Agents Chemother **43:**1329-1333.

17. **Gumbo T, Dona CS, Meek C, Leff R.** 2009. Pharmacokinetics-pharmacodynamics of pyrazinamide in a novel in vitro model of tuberculosis for sterilizing effect: a paradigm for faster assessment of new antituberculosis drugs. Antimicrob Agents Chemother **53:**3197-3204.

18. **Ahmad Z, Tyagi S, Minkowsk A, Almeida D, Nuermberger EL, Peck KM, Welch JT, Baughn AS, Jacobs WR, Grosset JH.** 2012. Activity of 5-chloro-pyrazinamide in mice infected with Mycobacterium tuberculosis or Mycobacterium bovis. Indian J Med Res **136:**808-814.

19. **Almeida DV, Tyagi S, Li S, Wallengren K, Pym AS, Ammerman NC, Bishai WR, Grosset JH.** 2014. Revisiting Anti-tuberculosis Activity of Pyrazinamide in Mice. Mycobact Dis **4:**145.

20. **Rullas J, García JI, Beltrán M, Cardona PJ, Cáceres N, García-Bustos JF, Angulo-Barturen I.** 2010. Fast standardized therapeutic-efficacy assay for drug discovery against tuberculosis. Antimicrob Agents Chemother **54:**2262-2264.

21. **Davis SL, Nuermberger EL, Um PK, Vidal C, Jedynak B, Pomper MG, Bishai WR, Jain SK.** 2009. Noninvasive pulmonary [18F]-2-fluoro-deoxy-D-glucose positron emission tomography correlates with bactericidal activity of tuberculosis drug treatment. Antimicrob Agents Chemother **53:**4879-4884.

22. **Harper J, Skerry C, Davis SL, Tasneen R, Weir M, Kramnik I, Bishai WR, Pomper MG, Nuermberger EL, Jain SK.** 2012. Mouse model of necrotic tuberculosis granulomas develops hypoxic lesions. J Infect Dis **205:**595-602.

23. **Driver ER, Ryan GJ, Hoff DR, Irwin SM, Basaraba RJ, Kramnik I, Lenaerts AJ.** 2012. Evaluation of a mouse model of necrotic granuloma formation using C3HeB/FeJ mice for testing of drugs against Mycobacterium tuberculosis. Antimicrob Agents Chemother **56:**3181-3195.

24. **Lanoix JP, Lenaerts AJ, Nuermberger EL.** 2015. Heterogeneous disease progression and treatment response in a C3HeB/FeJ mouse model of tuberculosis. Dis Model Mech **8:**603-610.

25. **Klinkenberg LG, Lee JH, Bishai WR, Karakousis PC.** 2010. The stringent response is required for full virulence of Mycobacterium tuberculosis in guinea pigs. J Infect Dis **202:**1397-1404.

26. **Larsen MH, Biermann K, Tandberg S, Hsu T, Jacobs WR.** 2007. Genetic Manipulation of Mycobacterium tuberculosis. Curr Protoc Microbiol **Chapter 10:**Unit 10A.12.

27. **Ioerger TR, Feng Y, Ganesula K, Chen X, Dobos KM, Fortune S, Jacobs WR, Mizrahi V, Parish T, Rubin E, Sassetti C, Sacchettini JC.** 2010. Variation among genome sequences of H37Rv strains of Mycobacterium tuberculosis from multiple laboratories. J Bacteriol **192:**3645-3653.

28. **Via LEaSRaWDMaZMDaPBaISMaLEaOBPa.** 2015. Host-Mediated Bioactivation of Pyrazinamide: Implications for Efficacy, Resistance, and Therapeutic Alternatives. ACS Infectious Diseases **1:**203-214.

29. **Andreas Sandgren.** 2015. Tuberculosis drug resistance data base. http://www.tbdreamdb.com/PZA_Rv2043c_AllMutations.html. Accessed March 9.

30. **Miotto P, Cabibbe AM, Feuerriegel S, Casali N, Drobniewski F, Rodionova Y, Bakonyte D, Stakenas P, Pimkina E, Augustynowicz-Kopeć E, Degano M, Ambrosi A, Hoffner S, Mansjö M, Werngren J, Rüsch-Gerdes S, Niemann S, Cirillo DM.** 2014. Mycobacterium tuberculosis pyrazinamide resistance determinants: a multicenter study. MBio **5:**e01819-01814.

31. **Donald PR, Maritz JS, Diacon AH.** 2012. Pyrazinamide pharmacokinetics and efficacy in adults and children. Tuberculosis (Edinb) **92:**1-8.

32. **Kjellsson MC, Via LE, Goh A, Weiner D, Low KM, Kern S, Pillai G, Barry CE, Dartois V.** 2012. Pharmacokinetic evaluation of the penetration of antituberculosis agents in rabbit pulmonary lesions. Antimicrob Agents Chemother **56:**446-457.

33. **Dartois V.** 2014. The path of anti-tuberculosis drugs: from blood to lesions to mycobacterial cells. Nat Rev Microbiol **12:**159-167.

34. **Prideaux B, Via LE, Zimmerman MD, Eum S, Sarathy J, O'Brien P, Chen C, Kaya F, Weiner DM, Chen PY, Song T, Lee M, Shim TS, Cho JS, Kim W, Cho SN, Olivier KN, Barry CE, Dartois V.** 2015. The association between sterilizing activity and drug distribution into tuberculosis lesions. Nat Med.

35. **Kiem S, Schentag JJ.** 2008. Interpretation of antibiotic concentration ratios measured in epithelial lining fluid. Antimicrob Agents Chemother **52:**24-36.

36. **Ahmad Z, Fraig MM, Bisson GP, Nuermberger EL, Grosset JH, Karakousis PC.** 2011. Dose-dependent activity of pyrazinamide in animal models of intracellular and extracellular tuberculosis infections. Antimicrob Agents Chemother **55:**1527-1532.

627 37. **Schaible UE, Sturgill-Koszycki S, Schlesinger PH, Russell DG.** 1998. Cytokine activation leads to
628 acidification and increases maturation of Mycobacterium avium-containing phagosomes in murine
629 macrophages. J Immunol **160:**1290-1296.
630 38. **Jayaraman S, Song Y, Verkman AS.** 2001. Airway surface liquid pH in well-differentiated airway
631 epithelial cell cultures and mouse trachea. Am J Physiol Cell Physiol **281:**C1504-1511.
632 39. **Bodem CR, Lampton LM, Miller DP, Tarka EF, Everett ED.** 1983. Endobronchial pH. Relevance of
633 aminoglycoside activity in gram-negative bacillary pneumonia. Am Rev Respir Dis **127:**39-41.
634 40. **WEISS C, TABACHNICK J, COHEN HP.** 1954. Mechanism of softening of tubercles. III. Hydrolysis
635 of protein and nucleic acid during anaerobic autolysis of normal and tuberculous lung tissue in vitro.
636 AMA Arch Pathol **57:**179-193.
637 41. **Weiser OL, Dye WE.** 1956. Assay of Streptomycin in resected lung tissue. Conference on the
638 chemotherapy of tuberculosis **12:**198-201.
639 42. **Fox W.** 1981. Whither short-course chemotherapy? Br J Dis Chest **75:**331-357.
640 43. **Mitchison DA.** 2000. Role of individual drugs in the chemotherapy of tuberculosis. Int J Tuberc
641 Lung Dis **4:**796-806.
642 44. **Aono A, Chikamatsu K, Yamada H, Kato T, Mitarai S.** 2014. Association between pncA gene
643 mutations, pyrazinamidase activity, and pyrazinamide susceptibility testing in Mycobacterium
644 tuberculosis. Antimicrob Agents Chemother **58:**4928-4930.
645 45. **Timm J, Kurepina N, Kreiswirth BN, Post FA, Walther GB, Wainwright HC, Bekker LG, Kaplan G,**
646 **McKinney JD.** 2006. A multidrug-resistant, acr1-deficient clinical isolate of Mycobacterium tuberculosis is
647 unimpaired for replication in macrophages. J Infect Dis **193:**1703-1710.
648 46. **Tan S, Sukumar N, Abramovitch RB, Parish T, Russell DG.** 2013. Mycobacterium tuberculosis
649 responds to chloride and pH as synergistic cues to the immune status of its host cell. PLoS Pathog
650 **9:**e1003282.
651 47. **Irwin SM, Gruppo V, Brooks E, Gilliland J, Scherman M, Reichlen MJ, Leistikow R, Kramnik I,**
652 **Nuermberger EL, Voskuil MI, Lenaerts AJ.** 2014. Limited Activity of Clofazimine as a Single Drug in a
653 Mouse Model of Tuberculosis Exhibiting Caseous Necrotic Granulomas. Antimicrob Agents Chemother
654 **58:**4026-4034.

655

656

657 **Tables and Figures**

658 Table 1: Plasma PK parameters of PZA in C3HeB/FeJ mice

Infection status	PZA dose (mg/kg)	AUC_{0-24} (µg.h/ml)	C_{max} (µg/ml)	$T_{1/2}$ (h)
Uninfected C3HeB/FeJ mice (single dose)	10	9.2	5.6	0.6
	30	59.2	23	1
	150	577.9	187.8	1.4
	300	1,081.6	263	1.9
	450 BID	5,326.8	665.3	3.5
Infected C3HeB/FeJ mice (steady state)	150	455.6	166	1.3
	450 BID	3,589.6	467	1.6
Infected BALB/c mice (single dose)	150 (28)	388	163	1.2
	450 BID*	3241.8	472.9	2.3

659 Legend: Parameters were calculated from mean concentration data. The data presented are

660 from one of two representative experiments in each infection condition. *= unpublished data

661

662

663 Table 2: Ratio of ELF/plasma PZA concentrations in C3HeB/FeJ mice.

	PZA dose (mg/kg)	Time Median ELF/plasma ratio (number of mice)			
		1.5h	3h	7h	12h
Uninfected mice (single dose)	30		1.2 (2)	3.7 (1)	
	150		0.9 (7)	1 (4)	22.8 (4)
	300		2 (6)	1 (5)	
	450 BID		1.1 (3)	2.2 (3)	1.2 (3)
Infected mice (steady state)	150	1.1 (6)	3 (7)	3.1 (8)	NA
	450 BID	1.3 (6)	1.6 (8)	1.2 (7)	

Legend: NA=not applicable (due to non-quantifiable PZA concentration in ELF or in plasma). No PZA was measurable at 0h and 17h time point or in the 10mg/kg arm.

668 Table 3: Results of mutations in *pncA* gene (Rv2043c) observed in PZA-resistant isolates

Type of mutation	BALB/c mouse strain	C3HeB/FeJ mouse strain	
Point mutations	K96M	M1I	T135P
	G132A	L19R	H137D
	C138Y	A46E	V139M
	T142P	S67P	A146V
	L159V	H71Y	S164P
	H171R	C72F	L172P
		Y99stop	E173stop
		G108R	
		I133N	
Small Indels*	+A in E127	-G in P54,	
		-CG in A26,	
		-T in I133	
		-CGTCAGCGGTACTC in V73-P77	
Large-scale Deletions	Rv2023c-Rv2048c (27 kb)	Rv2030c-Rv2048c (21 kb)	
	Rv2027c-Rv2047c (19.8 kb)	Rv2034-Rv2045c (9 kb)	
		Rv2039c-Rv2048c (13 kb)	
		Rv2040c-Rv2045c (3.5 kb)	
		Rv2041c-Rv2043c (1.1 kb)	

		Rv2042c-Rv2043c (1 kb) Rv2043c-Rv2044c (0.2 kb)
5' UTR	A>G -11 bp upstream	
No mutation	-	one (A3311T mutation in Rv3350c)

669 Legend: *frame-shifts

670

671 Figure 1

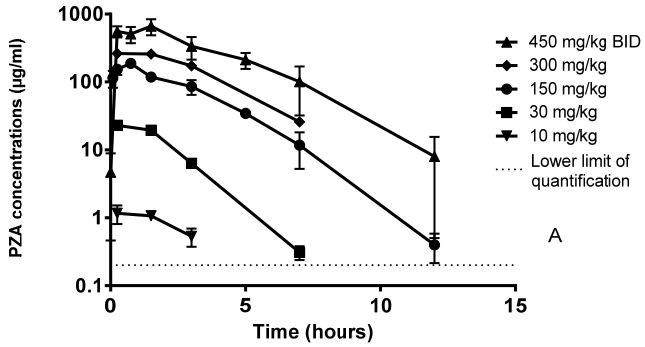

672

673 Legend: Dose-ranging PZA concentration-time profiles in uninfected C3HeB/FeJ mice in plasma.

674 Data are plotted as mean and SD.

675

676

677

678

679 Figure 2

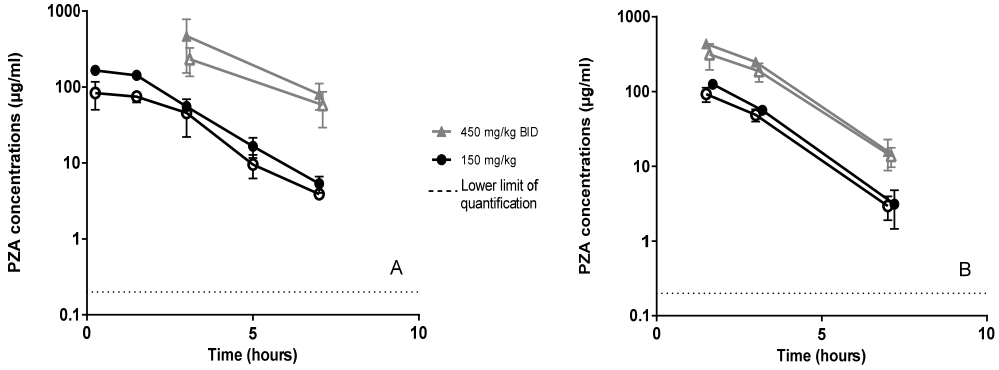

680

681 Legend: Dose-ranging PZA concentration-time profiles in infected C3HeB/FeJ mice in plasma

682 (solid shapes) and lesions (open shapes) for 150 and 450 BID mg/kg. Panel A and panel B

683 represents 2 different sets of experiment. Data are plotted as mean and SD.

684

685 Figure 3

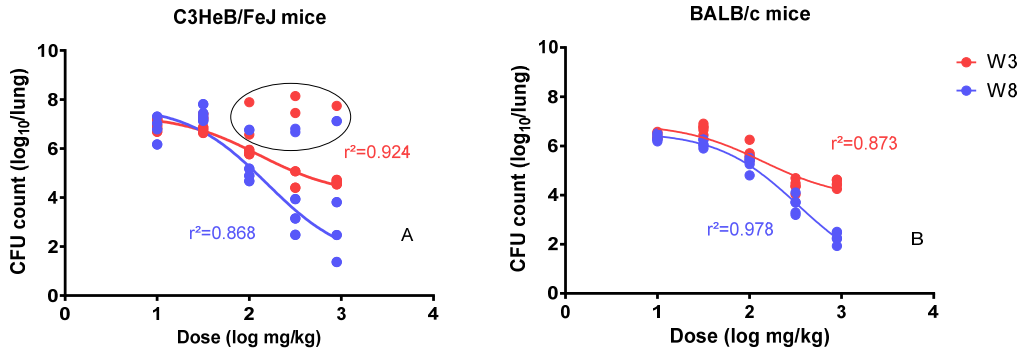

686

687 Legend: Dose-response profiles in C3HeB/FeJ mice (panel A) and BALB/c mice (panel B) after 3
688 weeks (blue symbols and line) and 8 weeks (red symbols and line) of treatment (W3 and W8
689 respectively). Open ellipse: C3HeB/FeJ mice excluded from curve fit (outliers).

690

691 Figure 4

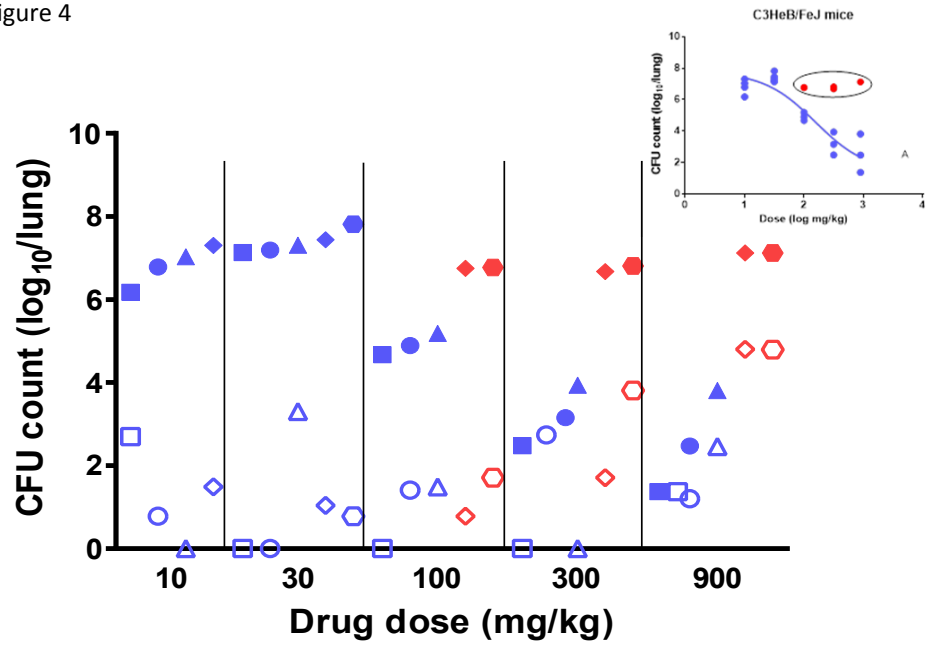

692

693 Legend: Total CFU counts (solid symbols) and PZA-resistant CFU counts (open symbols) in
694 C3HeB/FeJ mice treated with escalating PZA doses. Each symbol shape represents an individual
695 mouse in its dose group. Shown in blue are the CFU counts from mice considered to fit the
696 dose-response curve shown in the inset. Shown in red are the CFU counts from mice considered
697 non-responsive to the dose increase. Solid symbols indicate the total CFU counts determined on

698 drug-free media for each individual mouse. The open symbols indicate the resistant CFU counts

699 determined on PZA-containing plates for the same mouse.